Letters in Applied NanoBioScience
Open-Access Journal (ISSN: 2284-6808)

Review
Volume 12, Issue 4, 2023, 94
https://doi.org/10.33263/LIANBS124.094

Methods of Chitosan Identification: History and Trends

Izabela Dziedzic [1,2,*], Ahmet Kertmen [2,*]

[1] Faculty of Chemistry, Adam Mickiewicz University, Uniwersytetu Poznańskiego 8, 61-614 Poznan, Poland; izabela.dziedzic@amu.edu.pl (I.D.)
[2] Center for Advanced Technologies, Adam Mickiewicz University, Uniwersytetu Poznańskiego 10, 61-614 Poznan, Poland; ahmker@amu.edu.pl (A.K.)
* Correspondence: izadzi@amu.edu.pl (I.D.); ahmker@amu.edu.pl (A.K.);

Scopus Author ID 57216478956
Received: 7.06.2022; Accepted: 12.07.2022; Published: 17.09.2022

Abstract: Chitosan, discovered in 1859 and named in 1894, has long attracted the attention of scientists. However, endless possibilities for the chemical engineering of chitosan still offer inspiration for various innovative applications. The highly biocompatible and antimicrobial features of chitosan enable its multi-disciplinary applications, such as in medical engineering, food science, environmental science, and cosmetics; this is evident from the significantly increasing number of chitosan articles in the last two decades. This article presents methods for identifying chitosan using various analytical techniques and summarizes the findings from such techniques throughout the literature. The summary of the key analytical data presented in this review article could be used as a quick reference for a researcher who intends to analyze chitinous content by the method of their choice.

Keywords: chitosan; identification; methods.

1. Introduction

Chitosan is derivative of chitin which is, after cellulose, the second most abundant polysaccharide [1,2]. Chitin is a linear homopolymer composed of β-1,4-linked N-acetyl-D-glucosamine units [3] that have been identified within diverse skeletal structures of fungi [4], diatoms [5], and a broad diversity of invertebrates, including sponges [6–9], corals [10,11] as well as arthropods [12–16]. This structural amino polysaccharide is insoluble in aqueous solutions; however, when deacetylated, it becomes soluble in acidic solutions and is called chitosan [2]. It was produced for the first time in 1859 by the physiologist Charles Rouget from France (for details, see [17]). He discovered that after boiling chitin in a concentrated solution of potassium hydroxide, it could be soluble in dilute organic acid solutions. Rouget described the process of chitin deacetylation for the first time and called the product "modified chitin". German scientist Felix Hoppe-Seyler introduced the name "chitosan" in 1894 [17]. The molecule is protonated in the acidic pH amine group in the chitosan and makes the particle soluble [18]. The chitosan solubility depends on the acetylation degree and molecular weight [19]. Chitin and chitosan structures are presented in Figure 1.

Chitosan does not have every monomer unit deacetylated. But it contains chitin to some extent, which means that some units stay acetylated. It is possible to isolate more homogenous chitosan using carbohydrate-binding modules specific to chitosan. They are also useful for studying chitosan localization in biological tissues [20].

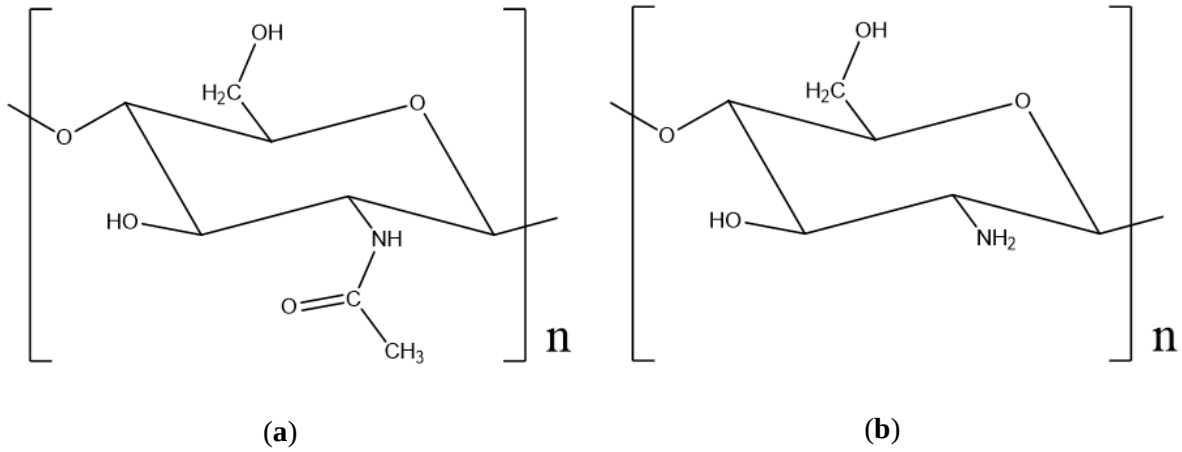

(a) **(b)**

Figure 1. Structure of: (a) chitin made of N-acetyl-β-D-glucosamine repeating units; (b) chitosan made of D-glucosamine units (adapted from [2]).

Chitin and chitosan remain great players in biomedicine due to their biodegradability, biocompatibility, and cell adhesion [21,22]. Chitosan is characterized by antimicrobial and antibacterial properties [18,23]. Among many biomedical applications, it should be noted that chitosan and its derivatives can be used for tissue engineering [24–27], drug delivery [28–33], or wound dressing [34–42]. Besides biomedicine chitosan is also used in cosmetics [43–45], biomineralization research [46,47], supercapacitors [48], water treatment [49–52], and food industry [53] as food packaging [54–57]. It is not surprising that such effective use of chitosan for medical and technological purposes stimulates analytical studies aimed at its identification and characterization.

This review presents the pool of chitosan identification methods, including physicochemical, structural, and spectroscopical approaches. It is the methods of identification, rather than characterization of chitosan, that are the main topic of our analytical review.

2. Spectroscopic and structural methods

2.1. Nuclear magnetic resonance spectroscopy (NMR).

NMR spectroscopy is a powerful method for analyzing organic compounds, including chitosan [58]. This technique is based on the possession of magnetic moment by some nuclei [59].

Both proton and carbon NMR methods are useful in chitosan identification.

The chemical shifts change with the deacetylation degree both in the ^{1}H NMR and ^{13}C NMR spectroscopy [60]. The approximated values of ^{1}H NMR and ^{13}C NMR chemical shifts are shown in Tables 1 and 2, respectively. Figure 2 presents the ^{1}H NMR spectrum of chitosan.

Table 1. ^{1}H NMR chemical shifts of chitosan [61].

Position	H1	H2	H3, H4, H5, H6	N-acetyl
δ (ppm)	4.8	3.1	3.6-3.8	2.0

Table 2. ^{13}C NMR chemical shifts of chitosan [61].

Position	C1	C2	C3	C4	C5	C6
δ (ppm)	100	60	73	80	78	63

NMR spectroscopy allows for the assessment of acetylation patterns. This is done using HOBS - Homodecuopled Band-Selective NMR, splitting into signals assigned with the

multivariate Pure Shift NMR method. Thus, acetylation patterns can be easily determined on various chitosan samples [62].

The time-domain NMR relaxometry with the pulse sequence Rhim and Kessemeier - Radio-frequency Optimized Solid-Echo (RK-ROSE) can be used to obtain the 1H NMR signal of solid-state materials. The RK-ROSE pulse sequence can support classical methods for determining the degree of acetylation and the crystallinity index, which may be useful for distinguishing chitosan samples with a similar degree of acetylation and possibly different crystallinity or even chitosan with a completely different degree of acetylation. The decay of the time-domain NMR signal may be advantageous in predicting trends in the structural and morphological features of the chitosan powder [63].

^{1}H NMR spectroscopy method also allows determining the deacetylation degree [64,65].

The degree of deacetylation can be calculated using the ratio of areas of the peak from the hydrogen atom in the acetyl group and the peak of the CH groups [66] or to the peak of the hydrogen atom bonded to the carbon having amine group [67].

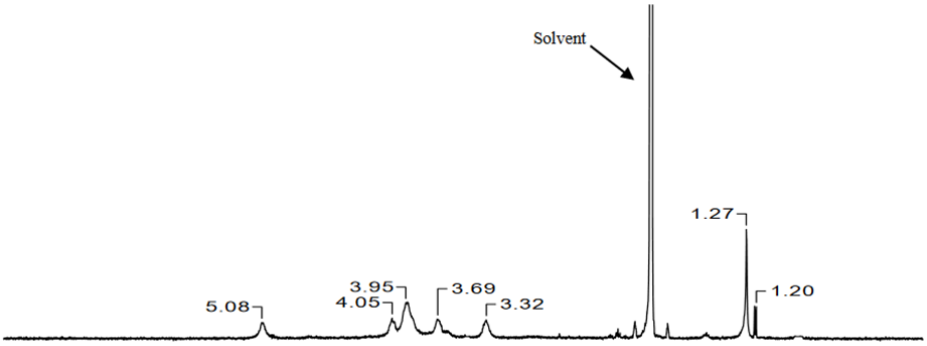

Figure 2. The ^{1}H NMR spectrum of chitosan [68].

2.2. X-ray diffraction spectroscopy (XRD).

XRD technique allows for analysis of the structure on the atomic scale [69]. Using this method, it is possible to find the atomic arrangement in the unit cell by data regression [70].

On the XRD diffractogram, chitosan exhibits two main peaks at about 10° and 20° 2θ angle values (Figure 3). These peaks indicate conformational and structural properties and chitosan's high degree of crystallinity [61,71]. The first peak is related to plane 020 (amine I – acetylated amine group of chitosan), and the second one is attributed to plane 110 (amine II – free amine group in chitosan) [72]. The 020 reflections are assigned to acetamide groups that can create hydrogen bonds with water and produce hydrated crystals [73]. The peak around 20° 2θ angle values is related to the chitosan crystal lattice, the orthorhombic unit cell [74]. On the diffractogram, there is also a smaller peak at 21° associated with a 120 plane. However, the XRD pattern of β-chitosan doesn't exhibit a peak at 2θ ≈ 10° because of the weak intermolecular force. Chitosan nanoparticles also don't show a peak at about 10°, and the peak at 20° becomes weak and wide, indicating crystal structures being in the amorphous state [72]. As the deacetylation degree increases, the peak at 10° shifts to higher values, and its intensity decreases. In comparison, the peak at 20° shifts to the lower values of the 2θ angle, and its intensity decreases [66,75].

Wide angle XRD analysis shows that chitosan with a low degree of deacetylation with a value higher than 24% is characterized by a different crystalline structure than chitin [76] and a different network of hydrogen bonds [77].

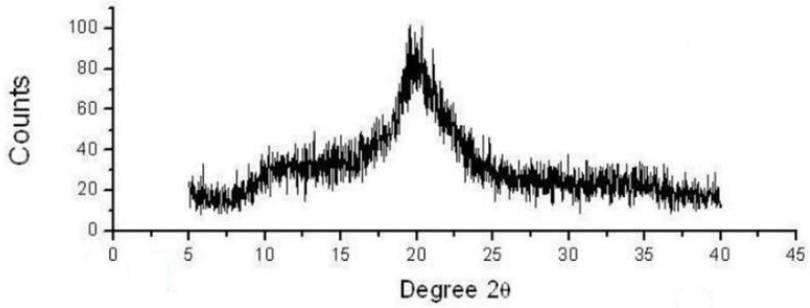

Figure 3. The XRD pattern of pure chitosan [78].

The peak at 10°, related to the 020 plane, moves to a higher angle and decreases with the increase of the degree of deacetylation. The crystalline index of this plane exhibits a linear relationship with the degree of deacetylation. This makes it possible to use the XRD technique to determine the deacetylation degree of macromolecular chitosan and chitin [75].

The chitosan fibers, after N-acylation, have their crystalline structure altered. The peak at 2θ = 10° on the XRD diffractogram is sharpened with the increasing chain length of the acyl group [79]. The change of the acetyl group content results in the expansion of the crystal lattice. N-deacetylation and N-acetylation cause a decrease in the crystallinity of chitosan or chitin [80]. Chitosan crystalline structure is destroyed in the milling process [81].

2.3. X-ray photoelectron spectroscopy (XPS).

XPS is an analytical method for surface analysis of the material. X-rays bombard the surface, and the released electrons' kinetic energy is measured [82].

This method identifies the sorption sites in the chitosan molecule [83]. XPS can determine the bonding energy of atoms on the chitosan surface and its chelate with metals. XPS is also useful in ascertaining the coordination number of the complexes of chitosan with metal [84].

XPS analysis of chitosan shows carbon, nitrogen, and oxygen atoms. Nitrogen 1s narrow scan exhibits two peaks of about 400 eV associated with amine and amide groups. Percentage atomic ratios of those peaks enable calculating the acetylation degree of chitosan [85]. The degree of deacetylation can be determined using XPS based on the nitrogen content change [86]. The atomic percentages of the elements can be calculated based on the integrated intensities of the XPS peaks [87]. The carbon 1s spectrum displays four peaks. First at 286 eV associated with carbon atom bonded to the amine group, second at approximately 287 eV attributed to carbon atoms linked to ether and hydroxyl group, next at 288 eV from atoms forming a glycosidic bond, last at 289 eV comes from carbon attached to amide group. Other peaks can be assigned to impurities [88].

Oxygen 1s spectrum of chitosan film exhibits a peak at approximately 533 eV and 534 eV. The former is attributed to oxygen in the hydroxyl group – linked with hydrogen and carbon atoms, the latter to the oxygen atom connected only with carbon atoms like in the ether group [89].

2.4. Fourier transform infrared spectroscopy (FT-IR).

Infrared spectroscopy is a very important analytical technique when working with chitosan. It is based on the vibrations of the atoms in the molecule when using infrared electromagnetic radiation. Fourier transform is a mathematical process that improves the

quality of the spectra [58]. FTIR spectrum of chitosan exhibits bands shown in Table 3. The spectrum is shown in Figure 4.

Table 3. IR bands of chitosan powder and its assignments [85,89].

Wavenumber (cm^{-1})	Peak assignment
3345	N-H symmetric stretching
3315 - 3215	N-H asymmetric stretching overlapping O-H stretching
2864	C-H stretching
1648	Amide I
1594	Amide II
1573	N-H bending from an amine
1414	CH_2 bending
1375	CH_3 symmetrical deformation
1150	C-O-C antisymmetrical stretching and C-N stretching
1026	C-O stretching skeletal vibrations
700 - 500	N-H wagging and O-H wagging

The degree of deacetylation can be determined using FTIR spectroscopy in several ways. One of them is comparing areas of the C=O peak from amide, which changes with the number of acetylated groups in chitosan particle, with the non-changing C—H peak. Baseline location is very important; for better results, the peak areas shouldn't be set too close. Another method is based on the peak maxima. First, the C—O—C peak is normalized to value 1. Then, the absolute height of C=O, N—H, and C—H peaks is used for forming linear equations and finally for calculating the degree of deacetylation. Another method is peak deconvolution. The degree of deacetylation is calculated by the integrals of the areas of the peaks deforming and stretching C — H [66]. Amide I band is more intense when the deacetylation degree is lower [90].

Chitosan from shrimp shells and chitosan from fungi exhibit the same characteristic peaks on the IR spectra. However, fungal chitosan presents a peak that is not seen in the chitosan from shrimps (around 1640 cm^{-1}) [91]. Chitosan beads exhibit a generally similar FTIR spectrum to chitosan but are slightly different. NH_3 peak around 1450 cm^{-1} is wider in chitosan beads [92].

Glucosamine and its chlorhydrate form do not exhibit any differences in the IR spectra. This can mean that in the dried state, protonation of the sample does not influence the spectrum. Also, water content does not influence the size of the -OH band at 3350 cm^{-1} [93].

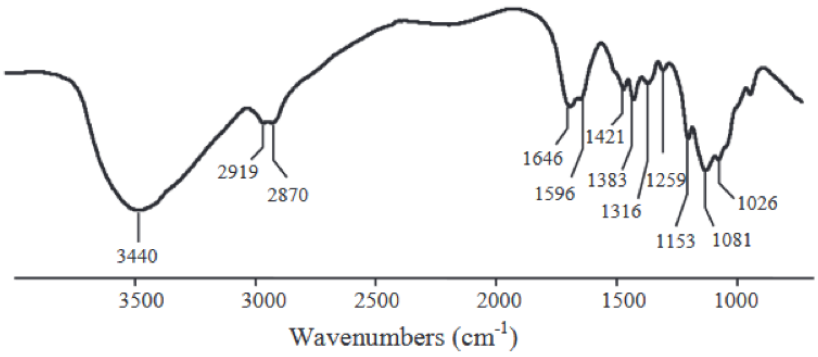

Figure 4. The IR spectrum of chitosan [68].

FTIR spectra of α- and β-chitin exhibit differences due to different hydrogen bonds. The spectrum of α-chitin shows two separated peaks at 1630 and 1662 cm^{-1} related to intramolecular hydrogen bonds –CO···$HOCH_2$– and –CO···HN–. On the contrary, the spectrum of β-chitin presents one peak at 1659 cm^{-1} attributed to the carbonyl group bonded to the amide group by a hydrogen bond. The amide bands at 3110 and 3264 cm^{-1} are distinct and clear in α-

chitin but weak in the β-chitin spectrum [94]. In chitosan's spectrum, peaks at 3265, 3105, and 1662 cm^{-1} disappear. However, the peak related to primary amide at 1596 cm^{-1} appears. These differences are better seen when β-chitin is deacetylated [95]. The characteristic marker is the CH deformation of β-1-4 glycosidic linkage is a band that shifts from 895 cm^{-1} in α-chitin to 890 cm^{-1} in β-chitin [3]. The chitosan peak at 1153 cm-1 is related to the β-1-4 glycosidic bond [96].

IR technique is useful for checking the protection of amine groups. It is a convenient and simple chemoselective method based on the reaction of chitosan with phthalic anhydride in N,N-dimethylformamide (DMF), which results in the production of N-phthaoloylchitosan. The presence of this imide can be confirmed using IR spectroscopy. The IR spectrum exhibits twin absorption peaks at 1712 and 1776 cm^{-1} [97].

2.5. Raman spectroscopy (RS).

In Raman spectroscopy monochromatic laser beam interacts with the sample particles and produces a scattered light. Scattered light with a frequency other than incident light is used to form the Raman spectrum [98].

Raman spectra exhibit peaks shown in table 4.

Table 4. Raman shifts of chitosan and its assignments [77,99–101].

Wavenumber (cm^{-1})	Peak assignment
2885	CH_2 stretching
1654	C-O stretching
1591	N-H deforming
1456	C-H and O-H bending
1324	C-N stretching
1146	C-O-C stretching
1109	C-OH stretching
936	C-N stretching

Chitin exhibit two peaks at 2882 and 2937 $cm^{-1,}$ while chitosan shows one peak at 2885 cm^{-1}. The peak at 2937 cm^{-1} can be attributed to C—H stretching vibrations in the acetyl group. The bands at 2882 and 2885 cm^{-1} are ascribed to C—H stretching vibrations in the glucosamine units. The spectrum of chitin presents signals ascribed to amide at 1621 and 1660 cm^{-1}, while chitosan has only a band at 1591 cm^{-1} caused by the amine group [77].

The degree of deacetylation can be determined using Raman spectroscopy. The bands at 1621 and 1660 cm^{-1} can be assigned to the carbonyl C=O groups in acetyl groups involved in forming hydrogen bonds. Using the areas under these bands and thus the relative amount of the carbonyl groups in chitosan compared to pure chitin can be calculated [77].

2.6. Ultraviolet-visible spectroscopy (UV-Vis).

UV-Vis technique uses the phenomenon of electromagnetic radiation absorption from the ultraviolet/visible range and following the excitation of electrons to the state with higher energy. The absorption of this radiation is restricted by the presence of certain groups [58].

Chitosan solution in hydrochloric acid exhibits an absorption band at 201 nm [58]. It has been reported that chitosan nanoparticles show an absorption peak at 250 nm [102].

The chitosan deacetylation degree can be determined using the first UV-Vis derivative method. It is based on the presence of the acetyl groups and their absorbance intensity. Wu and Zivanovic described this method as follows: "*The chitin and chitosan samples have been dissolved in concentrated phosphoric acid and heated, and UV-Vis scans are taken. Acetyl-*

glucosamine exhibit an absorption peak from 190 to 220 nm. The first derivative UV-Vis values have been plotted against the acetylglucosamine concentrations, and the best linear regression is at 203 nm" [103].

The method for determining the content of chitosan in solution is based on the colored complex of chitosan and Cibacron Brilliant Red, which can be measured at 575 nm [104]. However, this method is not reproducible at low chitosan concentrations. The sensitivity of this method can be increased by changing the reagent composition and the ratio of dye solution and chitosan [105]. In another improved method, the solution is centrifuged from colloids, and the concentration of not complexed dye is measured. Consequently, the method's sensitivity is increased to 2 ppm [106].

2.7. Mass spectroscopy (MS).

Mass spectroscopy is a destructive method that allows for obtaining the mass of the compound. This is by measuring the ratio of the mass to the charge of the ion [58].

It was used for the first time in 1982 as pyrolysis-mass spectrometry [58]. The sample under study has been decomposed at a high temperature and analyzed. The mass spectrum of chitosan exhibits peaks in the range from m/z 40 to 150. The most intensive peaks are at m/z 40-45,59,67,80,94 [107].

Mass spectrometry can be used to determine the deacetylation degree. This is by using the combination of gas chromatography and mass spectrometry. The mass spectrum allows for identifying the volatile substances obtained from glucosamine and N-acetyl-glucosamine units. The peaks at m/z = 67 and 80 are derived from deacetylated units, while ions m/z = 42 and 60 are from acetylated monomers. The deacetylation degree is established based on the peak ratios [58].

2.8. Colorimetric assay (CA).

The colorimetric method is used to determine chitosan concentration in watery solutions quickly. This can be done by measuring the absorbance of the solutions and then plotting the analytical curve [108]. Figure 5 presents an example of the analytical curve for chitosan.

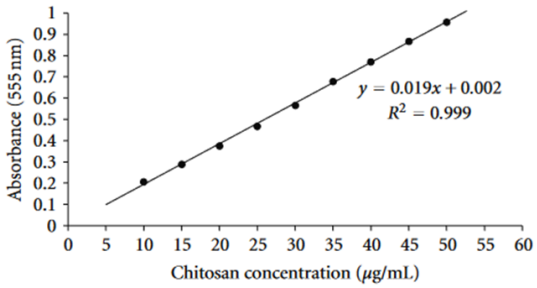

Figure 5. Example of the standard analytical curve for chitosan [109].

There is a variety of colorimetric methods for chitosan determination. One of them involves converting chitosan into 2,5-anhydro-D-mannose, which reacts with thiobarbituric acid giving pink color measured at 555 nm [109]. In a modification of this method, the thiobarbituric acid is replaced with DNSA – 3,5-dinitrosalicylic acid [110]. In addition, there is a method allowing chitosan determination in the presence of proteins [111]. A proposed

method also uses anionic dyes such as bromocresol green or bromocresolpurple, which form a colored complex product with chitosan [112].

The ninhydrin test is used to quantify free amine groups in the chitosan polysaccharide chain. The ninhydrin reacts with the chitosan's primary amine groups forming diketohydrindylidene-diketohydrindamin. The product is a colored substance measured in the spectrophotometer at 570 nm [113].

Chitosan, after hydrolysis, led to the formation of glucosamine, which can react with acetylacetone under alkaline conditions to form pyrrole, and then react with an acid alcohol solution of paradimethylaminobenzaldehyde to give the red product, which can be measured by spectrophotometry at 525 nm and determine the chitosan content [114].

Chitosan can be converted to an intermediate to produce a pink-colored product that can be detected at 532 nm. The absorbance intensity is proportional to the concentration of chitosan [115,116].

2.9. Elemental analysis (EA).

This technique allows for determining the number of certain elements in the sample. It is generally based on atomic absorption, fluorescence, and emission [117].

Chitosan contains approximately 40% of carbon, 7.5% of hydrogen, and 7.5% of nitrogen [118,119]. The weight percentage ratio of carbon and nitrogen enables the calculation of the deacetylation degree of the chitosan sample [66].

A higher degree of deacetylation is associated with an increase in nitrogen content and a decrease in carbon content [86]. The C/N ratio ranges from 5.145 for the fully N-deacetylated chitosan to 6.861 for the completely N-acetylated polymer. The percent of nitrogen in completely deacetylated chitosan is 8.7% and in fully acetylated chitin is 6.9% [120].

3. Thermo-analytical methods

3.1. Differential scanning calorimetry (DSC).

Differential scanning calorimetry is a thermal analysis method measuring how the substance's physical properties change over time with temperature. The measurement is based on the difference in the temperature of the reference material and the sample [121].

DSC thermogram of chitosan exhibits two peaks. The first one (endothermic, below 100°C) is associated with the loss of water molecules. The second signal (exothermic, approximately 300°C) is related to the decomposition of the chitosan pyranose ring [122–124]. The melting point of chitosan determined by the DSC method totals about 110°C [125].

3.2. Thermogravimetric analysis (TGA).

The thermogravimetric analysis uses mass loss processes in high temperatures that give information about composition, thermal stability, and extent of cure. What is measured is the mass of the polymer as a function of time or temperature [126].

This method allows for assessing the thermal stability of a substance and checking the weight change. Chitosan nanoparticles present two losses of weight. The first, from 50 to 110°C, is related to absorbed water loss. The second one, from 190 to 330°C is attributed to depolymerization and decomposition of the chitosan units or dehydration of the saccharide ring [127,128]. Solid and dissolved chitosan shows 5-8% weight loss below 100°C related to water

loss. In solid chitosan, at around 300°C there is about 50% weight loss associated with releasing oxygen-containing groups. As the deacetylation degree increases, the loss becomes greater. About 40% weight loss occurs in dissolved chitosan below 200°C. At the temperature of 350-480°C, the saccharide ring depolymerization and dehydration occur [66]. Figure 6 shows the thermogravimetric analysis of chitosan.

The first derivative of the TGA plot gives the derivative thermogravimetry thermogram (DTG), which presents degradation temperature. For chitosan nanoparticles, the DTG thermogram shows the first step of degradation at about 246°C and the second at about 330°C [127,128].

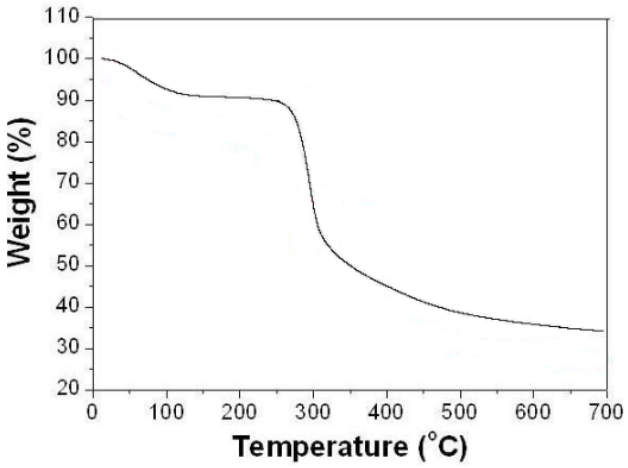

Figure 6. Thermogravimetric analysis of chitosan [78].

4. Other methods

4.1. Potentiometric and conductometric titration

For the titration, chitosan is dissolved in an acid and titrated with a base. The ending point of the titration is determined by an indicator or the conductance of the solution [113].

The degree of deacetylation can be determined by acid-base titration and pH measurement. Firstly, chitosan is dissolved in HCl, and KOH solution is added. The higher degree of deacetylation, the more volume of KOH is needed to neutralize the chitosan solution. The degree of deacetylation can be calculated based on the amount of the titrated amine groups with respect to the total amount of deacetylated and acetylated units [66,67].

The procedure is as in the potentiometric titration in conductometric, but the conductivity is measured. Using the titration curves, the number of moles of the amine groups can be calculated, and in consequence, the degree of deacetylation of chitosan [66,67].

4.2. Visual fluorescent identification.

This technique uses the strong affinity of a fluorescent agent to the amine group in chitosan. Then, the resulting fluorescent product can be visually recognized [129].

TSTPE – 1,1,2,2-tetrakis[4-(3-sulfonatopropoxyl)phenyl]-ethylene sodium salt is a fluorescent substance that can be added to hydrogels to identify chitosan. This salt is bounded by electrostatic interactions to chitosan's amino groups and exhibits fluorescence in blue color. After excitation at 360 nm, the hydrogels exhibit an emission spectrum presenting a peak at 480 nm, the intensity of which increases with an increasing degree of deacetylation [129].

4.3. High-performance liquid chromatography (HPLC).

HPLC technique separates the molecules based on their solubility in organic solvents or water, their charge, or their size. Then, the compounds can be identified and quantified [130].

This method is used for quantitative chitosan analysis. The chitosan is hydrolyzed in a strongly acidic environment to glucosamine salts, the concentration of which can be determined by HPLC. The higher the deacetylation degree of chitosan, the lower its hydrolysis rate. HPLC allows to the calculation of the actual chitosan content. This can be done using the hydrolysis rate of chitosan and ratio coefficient, which is based on the hydrolysis rates of chitosan and chitin [131]. The method combining acid hydrolysis and HPLC exhibits good precision and accuracy in determining the acetyl content, no matter the sample solubility. Hydrolysis of the oxalic acid and sulfuric acid at a temperature of 110°C during 30-40 min significantly increases the accuracy and precision. But the relative standard deviations are higher for chitosan with a high degree of deacetylation [132].

Because chitosan with aldehydes in Schiff base derivatives exhibits better hydrolysis than pure chitosan, it can be used for determining the chitosan content. The concentration of the product of the hydrolysis – glucosamine hydrochloride – has been determined by the HPLC, and its mass has been consequently calculated. The total chitosan content was calculated using the theoretical chitosan and the chitosan sample mass used in the Schiff base reaction. For this method, it is not necessary to purify and wash the derivative products before the hydrolysis [133].

The method to determine the chitosan in water and wood samples is based on acidic chitosan hydrolysis to glucosamine, derivatization with o-phthalaldehyde, chromatographic separation, and fluorescence detection [134].

4.4. Enzymatic method.

In the enzymatic method, enzymes such as chitinases or chitosanases degrade polymeric chitosans to oligosaccharides. Then, the degradation products can be analyzed [135].

This method allows for determining the very small amount of chitosan content in the sample. Chitinase is the enzyme that hydrolyses the cell wall of fungi. Then the amount of glucosamine is determined [136]. This method can be used to determine the deacetylation degree of chitosan. Firstly, chitosan is completely hydrolyzed by enzymes. Then the amount of glucosamine and N-acetylglucosamine is measured using the colorimetric assay or HPLC. Then the degree of deacetylation can be calculated [137].

4.5. Viscometric method.

The Viscometric technique measures the number of macromolecule agglomerates in solutions. The obtained viscosity values are a function of the degree of polymerization and chitosan content. This relationship can be used to determine the chitosan mass in solutions.

This method allows for determining the absolute concentration of chitosan. The method is also applicable if the chitosan concentration is low. As the polymerization degree decreases, the viscosity changes. The pH and concentration must be constant [138].

4.6. Van Wisselingh test.

This test is also called the „chitosan-iodine test for chitin". It is based on the hydrolysis of chitin to chitosan in the deacetylation process.

While natural chitin does not react in this reaction, chitosan reacts with iodine, giving brown colored adduct. For chitin, the color seems black, but after a more thorough examination, it is reddish-purple [3].

5. Trends and open questions

Using the Scopus database, the number of published articles every year was identified. Analysis of scholarly articles included title, abstract, and keywords. The search criteria consisted of "chitosan" and the above identification methods, namely NMR, XRD, XPS, FTIR, RS, UV-Vis, MS, DSC, TGA, SEM, CA, and EA. The results of the search are shown in Figure 7.

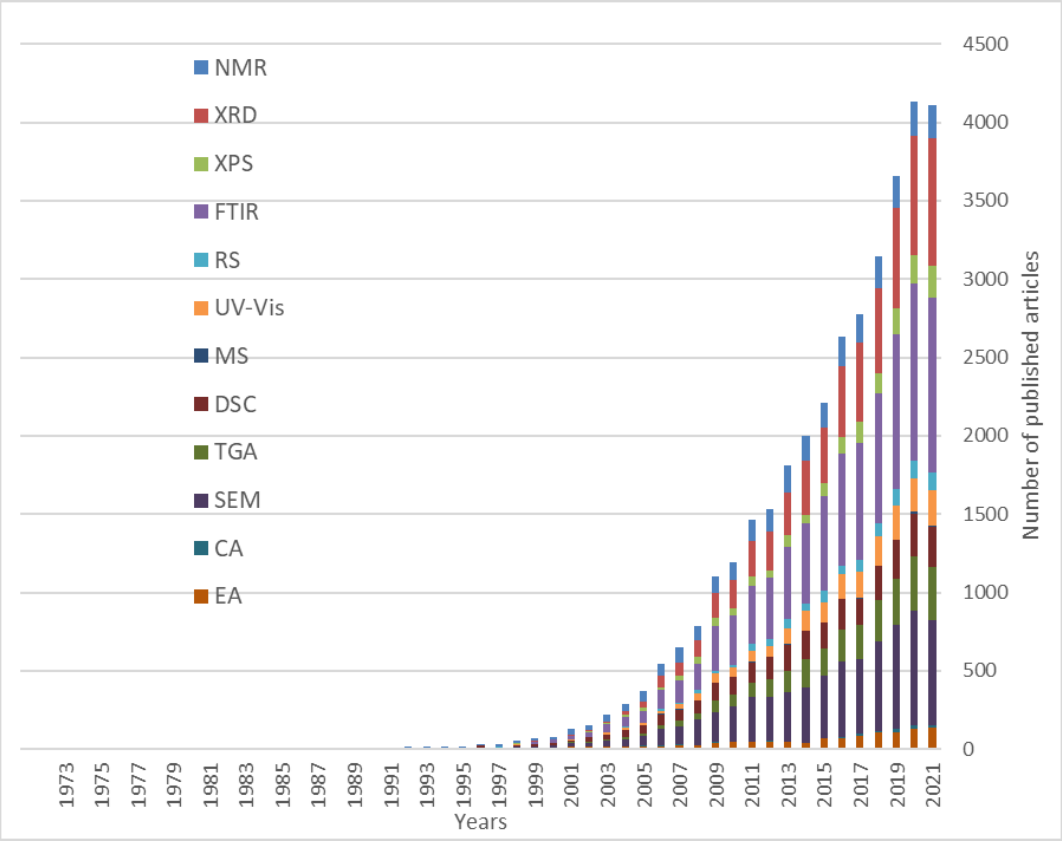

Figure 7. The plot shows the number of articles published each year containing chitosan and the method of identification.

The oldest article was published in 1972 using elemental analysis. The most commonly used method was FTIR, and the second was XRD.

One of the open questions concerning chitosan identification remains to be obtaining chitosan layers on 3D chitin scaffolds isolated from verongiid demosponges (see for an overview [11,139–146]. Recently, it has been reported [21] that "preliminary experiments with sponge chitin scaffolds using 47% NaOH at 85 ◦C showed, with strong evidence, that the outer layers of this chitin can be transformed into chitosan. The 3D architecture of the scaffolds remains stable after the surface deacetylation procedure. For future applications, however, the optimum degree of deacetylation needs to be determined" [21]. Such unique chitin-chitosan 3D hybrid constructs seem to be highly interesting for diverse applications in the fields of biomedicine and technology in the future, especially due to the renewability of poriferan chitin as a large scale production of marine sponges aquaculture [147,148].

6. Conclusions

A thorough analysis of the most widely used analytical techniques of chitosan characterization one more time demonstrated that the most important parameter for describing chitosan particles was the degree of deacetylation. Chitosan structure has been described by different parameters, such as the pattern of acetylation, fraction of acetylation, and degree of polymerization. While the degree of polymerization and fraction of acetylation of chitosan oligomers can be simply determined with nuclear magnetic resonance (NMR), mass spectrometry (MS), size-exclusion chromatography (SEC), thin-layer chromatography (TLC), or gel electrophoresis (GE); the pattern of acetylation can be most effectively determined by NMR method only when the oligomers are not too long. For short and non-complex oligomers, MS proves to be the method of choice. For chitosan polymers, the molecular weight can be determined by light scattering and viscosity calculation combined with size exclusion chromatography.

It has been evident from the SCOPUS keyword search that FTIR and XRD techniques have been the most frequently used techniques. In the case of FTIR, straightforward sample preparation combined with the possibility of differentiating alpha and beta-type chitinous materials stands out as the most obvious reason behind the popularity of the FTIR technique. On the contrary, the popularity of the XRD technique could be attributed to the vast availability of X-ray diffraction infrastructure that easily determines the occurrence of deacetylation in chitinous materials.

Funding

This research was funded by the National Science Centre within the framework of the project OPUS-19 No. 2020/37/B/ST5/01909.

Acknowledgments

This research has no acknowledgment.

Conflicts of Interest

The authors declare no conflict of interest.

References

1. Kertmen, A.; Ehrlich, H. Patentology of Chitinous Biomaterials. Part I: Chitin. *Carbohydr. Polym.* **2022**, *282*, https://doi.org/10.1016/j.carbpol.2022.119102.
2. Rinaudo, M. Chitin and Chitosan: Properties and Applications. *Prog. Polym. Sci.* **2006**, *31*, 603–632, https://doi.org/10.1016/j.progpolymsci.2006.06.001.
3. Tsurkan, M.V.; Voronkina, A.; Khrunyk, Y.; Wysokowski, M.; Petrenko, I.; Ehrlich, H. Progress in Chitin Analytics. *Carbohydr Polym* **2021**, *252*, https://doi.org/10.1016/j.carbpol.2020.117204.
4. Muzzarelli, R.; Boudrant, J.; Meyer, D.; Manno, N.; DeMarchis, M.; Paoletti, M. Current Views on Fungal Chitin/Chitosan, Human Chitinases, Food Preservation, Glucans, Pectins and Inulin: A Tribute to Henri Braconnot, Precursor of Thecarbohydrate Polymers Science, on the Chitin Bicentennial. *Carbohydr. Polym.* **2012**, *87*, 995–1012, https://doi.org/10.1016/j.carbpol.2011.09.063.
5. Brunner, E.; Richthammer, P.; Ehrlich, H.; Paasch, S.; Simon, P.; Ueberlein, S.; van Pée, K.-H. Chitin-Based Organic Networks: An Integral Part of Cell Wall Biosilica in the Diatom Thalassiosira Pseudonana. *Angew Chem Int Ed Engl* **2009**, *48*, 9724–9727, https://doi.org/10.1002/anie.200905028.
6. Ehrlich, H. Chitin and Collagen as Universal and Alternative Templates in Biomineralization. *Int. Geol. Rev.* **2010**, *52*, 661–699, https://doi.org/10.1080/00206811003679521.

7. Ehrlich, H.; Maldonado, M.; Spindler, K.-D.; Eckert, C.; Hanke, T.; Born, R.; Goebel, C.; Simon, P.; Heinemann, S.; Worch, H. First Evidence of Chitin as a Component of the Skeletal Fibers of Marine Sponges. Part I. Verongidae (Demospongia: Porifera). *J Exp Zool B Mol Dev Evol* **2007**, *308*, 347–356, https://doi.org/10.1002/jez.b.21156.
8. Klinger, C.; Żółtowska-Aksamitowska, S.; Wysokowski, M.; Tsurkan, M.V.; Galli, R.; Petrenko, I.; Machałowski, T.; Ereskovsky, A.; Martinović, R.; Muzychka, L.; Smolii, O.B.; Bechmann, N.; Ivanenko, V.; Schupp, P.J.; Jesionowski, T.; Giovine, M.; Joseph, Y.; Bornstein, S.R.; Voronkina, A.; Ehrlich, H. Express Method for Isolation of Ready-to-Use 3D Chitin Scaffolds from Aplysina Archeri (Aplysineidae: Verongiida) Demosponge. *Mar. Drugs* **2019**, *17*, https://doi.org/10.3390/md17020131.
9. Żółtowska, S.; Klinger, C.; Petrenko, I.; Wysokowski, M.; Joseph, Y.; Jesionowski, T.; Ehrlich, H. Methods of Isolating Chitin from Sponges (Porifera). In: *Chitin and Chitosan*. John Wiley & Sons, Ltd, **2019**; pp. 35–59, https://doi.org/10.1002/9781119450467.ch2.
10. Bo, M.; Bavestrello, G.; Kurek, D.; Paasch, S.; Brunner, E.; Born, R.; Galli, R.; Stelling, A.L.; Sivkov, V.N.; Petrova, O.V.; Vyalikh, D.; Kummer, K.; Molodtsov, S.L.; Nowak, D.; Nowak, J.; Ehrlich, H. Isolation and identification of chitin in the black coral Parantipathes larix (Anthozoa: Cnidaria). *International Journal of Biological Macromolecules* **2012**, *51*, 129-137, https://doi.org/10.1016/j.ijbiomac.2012.04.016.
11. Nowacki, K.; Stępniak, I.; Langer, E.; Tsurkan, M.; Wysokowski, M.; Petrenko, I.; Khrunyk, Y.; Fursov, A.; Bo, M.; Bavestrello, G.; Joseph, Y.; Ehrlich, H. Electrochemical Approach for Isolation of Chitin from the Skeleton of the Black Coral Cirrhipathes sp. (Antipatharia). *Marine Drugs* **2020**, *18*, https://doi.org/10.3390/md18060297.
12. Giraud-Guille, M.-M.; Chanzy, H.; Vuong, R. Chitin Crystals in Arthropod Cuticles Revealed by Diffraction Contrast Transmission Electron Microscopy. *J. Struct. Biol.* **1990**, *103*, 232–240, https://doi.org/10.1016/1047-8477(90)90041-A.
13. Jabeen, F.; Younis, T.; Sidra, S.; Muneer, B.; Nasreen, Z.; Saleh, F.; Mumtaz, S.; Saeed, R.F.; Abbas, A.S. Extraction of Chitin from Edible Crab Shells of *Callinectes Sapidus* and Comparison with Market Purchased Chitin. *Braz. J. Biol.* **2021**, *83*, https://doi.org/10.1590/1519-6984.246520.
14. Percot, A.; Viton, C.; Domard, A. Optimization of Chitin Extraction from Shrimp Shells. *Biomacromolecules* **2003**, *4*, 12–18, https://doi.org/10.1021/bm025602k.
15. Rødde, R.; Einbu, A.; Varum, K. A Seasonal Study of the Chemical Composition and Chitin Quality of Shrimp Shells Obtained from Northern Shrimp (Pandalus Borealis). *Carbohydr. Polym.* **2008**, *71*, 388–393, https://doi.org/10.1016/j.carbpol.2007.06.006.
16. Xie, J.; Xie, W.; Yu, J.; Xin, R.; Shi, Z.; Song, L.; Yang, X. Extraction of Chitin From Shrimp Shell by Successive Two-Step Fermentation of Exiguobacterium Profundum and Lactobacillus Acidophilus. *Front. Microbiol.* **2021**, *12*, https://doi.org/10.3389/fmicb.2021.677126.
17. Crini, G. Historical Review on Chitin and Chitosan Biopolymers. *Environ Chem Lett* **2019**, *17*, 1623–1643, https://doi.org/10.1007/s10311-019-00901-0.
18. Goy, R.C.; Britto, D. de; Assis, O.B.G. A Review of the Antimicrobial Activity of Chitosan. *Polímeros* **2009**, *19*, 241–247, https://doi.org/10.1590/S0104-14282009000300013.
19. Shepherd, R.; Reader, S.; Falshaw, A. Chitosan Functional Properties. *Glycoconj J* **1997**, *14*, 535–542, https://doi.org/10.1023/a:1018524207224.
20. Shinya, S.; Ohnuma, T.; Yamashiro, R.; Kimoto, H.; Kusaoke, H.; Anbazhagan, P.; Juffer, A.H.; Fukamizo, T. The First Identification of Carbohydrate Binding Modules Specific to Chitosan. *J Biol Chem* **2013**, *288*, 30042–30053, https://doi.org/10.1074/jbc.M113.503243.
21. Ehrlich, H. Chitin of Poriferan Origin as a Unique Biological Material. In: *Blue Biotechnology*. John Wiley & Sons, Ltd, Volume 1, **2018**; pp. 821–854, https://doi.org/10.1002/9783527801718.ch26.
22. Kertmen, A.; Ehrlich, H. Patentology of chitinous biomaterials. Part I: Chitin. *Carbohydrate Polymers* **2022**, *282*, https://doi.org/10.1016/j.carbpol.2022.119102.
23. Fei Liu, X.; Lin Guan, Y.; Zhi Yang, D.; Li, Z.; De Yao, K. Antibacterial Action of Chitosan and Carboxymethylated Chitosan. *J. Appl. Polym. Sci.* **2001**, *79*, 1324–1335, https://doi.org/10.1002/1097-4628(20010214)79:7<1324::AID-APP210>3.0.CO;2-L.
24. Croisier, F.; Jérôme, C. Chitosan-Based Biomaterials for Tissue Engineering. *Eur. Polym. J.* **2013**, *49*, 780–792, https://doi.org/10.1016/j.eurpolymj.2012.12.009.
25. Rajabi, M.; McConnell, M.; Cabral, J.; Ali, M.A. Chitosan Hydrogels in 3D Printing for Biomedical Applications. *Carbohydr. Polym.* **2021**, *260*, https://doi.org/10.1016/j.carbpol.2021.117768.
26. Maharjan, B.; Park, J.; Kaliannagounder, V.K.; Awasthi, G.P.; Joshi, M.K.; Park, C.H.; Kim, C.S. Regenerated Cellulose Nanofiber Reinforced Chitosan Hydrogel Scaffolds for Bone Tissue Engineering. *Carbohydr. Polym.* **2021**, *251*, https://doi.org/10.1016/j.carbpol.2020.117023.
27. Saatchi, A.; Arani, A.R.; Moghanian, A.; Mozafari, M. Synthesis and Characterization of Electrospun Cerium-Doped Bioactive Glass/Chitosan/Polyethylene Oxide Composite Scaffolds for Tissue Engineering Applications. *Ceram. Int.* **2021**, *47*, 260–271, https://doi.org/10.1016/j.ceramint.2020.08.130.
28. Jhaveri, J.; Raichura, Z.; Khan, T.; Momin, M.; Omri, A. Chitosan Nanoparticles-Insight into Properties, Functionalization and Applications in Drug Delivery and Theranostics. *Molecules* **2021**, *26*, https://doi.org/10.3390/molecules26020272.

29. Shi, W.; Ching, Y.C.; Chuah, C.H. Preparation of Aerogel Beads and Microspheres Based on Chitosan and Cellulose for Drug Delivery: A Review. *Int. J. Biol. Macromol.* **2021**, *170*, 751–767, https://doi.org/10.1016/j.ijbiomac.2020.12.214.
30. Hu, Q.; Luo, Y. Chitosan-Based Nanocarriers for Encapsulation and Delivery of Curcumin: A Review. *Int. J. Biol. Macromol.* **2021**, *179*, 125–135, https://doi.org/10.1016/j.ijbiomac.2021.02.216.
31. Shakeran, Z.; Keyhanfar, M.; Varshosaz, J.; Sutherland, D.S. Biodegradable Nanocarriers Based on Chitosan-Modified Mesoporous Silica Nanoparticles for Delivery of Methotrexate for Application in Breast Cancer Treatment. *Mater. Sci. Eng. C* **2021**, *118*, https://doi.org/10.1016/j.msec.2020.111526.
32. Tao, F.; Ma, S.; Tao, H.; Jin, L.; Luo, Y.; Zheng, J.; Xiang, W.; Deng, H. Chitosan-Based Drug Delivery Systems: From Synthesis Strategy to Osteomyelitis Treatment – A Review. *Carbohydr. Polym.* **2021**, *251*, https://doi.org/10.1016/j.carbpol.2020.117063.
33. Liang, Y.; Wang, Y.; Wang, L.; Liang, Z.; Li, D.; Xu, X.; Chen, Y.; Yang, X.; Zhang, H.; Niu, H. Self-Crosslinkable Chitosan-Hyaluronic Acid Dialdehyde Nanoparticles for CD44-Targeted SiRNA Delivery to Treat Bladder Cancer. *Bioact. Mater.* **2021**, *6*, 433–446, https://doi.org/10.1016/j.bioactmat.2020.08.019.
34. Rafieian, S.; Mahdavi, H.; Masoumi, M.E. Improved Mechanical, Physical and Biological Properties of Chitosan Films Using Aloe Vera and Electrospun PVA Nanofibers for Wound Dressing Applications. *J. Ind. Text.* **2021**, *50*, 1456–1474, https://doi.org/10.1177/1528083719866932.
35. Hassan, M.A.; Tamer, T.M.; Valachová, K.; Omer, A.M.; El-Shafeey, M.; Mohy Eldin, M.S.; Šoltés, L. Antioxidant and Antibacterial Polyelectrolyte Wound Dressing Based on Chitosan/Hyaluronan/Phosphatidylcholine Dihydroquercetin. *Int. J. Biol. Macromol.* **2021**, *166*, 18–31, https://doi.org/10.1016/j.ijbiomac.2020.11.119.
36. Yaşayan, G.; Karaca, G.; Akgüner, Z.P.; Bal Öztürk, A. Chitosan/Collagen Composite Films as Wound Dressings Encapsulating Allantoin and Lidocaine Hydrochloride. *Int. J. Polym. Mater. Polym. Biomater.* **2021**, *70*, 623–635, https://doi.org/10.1080/00914037.2020.1740993.
37. Prakash, C.; Sukumar, N.; Ramesh, P.; Kubera Sampath Kumar, S. Development and Characterization of Wound Dressing Material Coated with Natural Extracts of Curcumin, Aloe Vera and Chitosan Solution Enhanced with RhEGF (REGEN-DTM). *J. Nat. Fibers* **2021**, *18*, 2019–2032, https://doi.org/10.1080/15440478.2019.1710738.
38. Ebhodaghe, S.O. Hydrogel – Based Biopolymers for Regenerative Medicine Applications: A Critical Review. *Int. J. Polym. Mater. Polym. Biomater.* **2022**, *71*, 155–172, https://doi.org/10.1080/00914037.2020.1809409.
39. Naderi Gharehgheshlagh, S.; Fatemi, M.J.; Jamili, S.; Nourani, M.R.; Sharifi, A.M.; Saberi, M.; Amini, N.; Ganji, F. A Dermal Gel Made of Rutilus Kutum Skin Collagen-Chitosan for Deep Burn Healing. *Int J Pept Res Ther* **2021**, *27*, 317–328, https://doi.org/10.1007/s10989-020-10082-y.
40. Mansuroğlu, B.; Kızılbey, K.; Şayan Poyraz, F.; Yurttaş, Z.; Fuerkaiti, S.N.; Abaoğlu, İ.Y.; Başat, H.N. Chitosan/Dextran Sulphate Sodium Hydrogels for Wound Healing Material: Preparation, Characterisation and in Vitro Evaluation. *Mater Technol* **2021**, *36*, 843–850, https://doi.org/10.1080/10667857.2020.1800297.
41. Wang, X.-F.; Li, M.-L.; Fang, Q.-Q.; Zhao, W.-Y.; Lou, D.; Hu, Y.-Y.; Chen, J.; Wang, X.-Z.; Tan, W.-Q. Flexible Electrical Stimulation Device with Chitosan-Vaseline® Dressing Accelerates Wound Healing in Diabetes. *Bioact. Mater.* **2021**, *6*, 230–243, https://doi.org/10.1016/j.bioactmat.2020.08.003.
42. Moghadas, B.; Solouk, A.; Sadeghi, D. Development of Chitosan Membrane Using Non-Toxic Crosslinkers for Potential Wound Dressing Applications. *Polym. Bull.* **2021**, *78*, 4919–4929, https://doi.org/10.1007/s00289-020-03352-8.
43. Seino, H.; Kawaguchi, N.; Arai, Y.; Ozawa, N.; Hamada, K.; Nagao, N. Investigation of Partially Myristoylated Carboxymethyl Chitosan, an Amphoteric-Amphiphilic Chitosan Derivative, as a New Material for Cosmetic and Dermal Application. *J. Cosmet. Dermatol.* **2021**, *20*, 2332–2340, https://doi.org/10.1111/jocd.13833.
44. Sharkawy, A.; Barreiro, M.F.; Rodrigues, A.E. New Pickering Emulsions Stabilized with Chitosan/Collagen Peptides Nanoparticles: Synthesis, Characterization and Tracking of the Nanoparticles after Skin Application. *Colloids Surf. A: Physicochem. Eng. Asp.* **2021**, *616*, https://doi.org/10.1016/j.colsurfa.2021.126327.
45. Ta, Q.; Ting, J.; Harwood, S.; Browning, N.; Simm, A.; Ross, K.; Olier, I.; Al-Kassas, R. Chitosan Nanoparticles for Enhancing Drugs and Cosmetic Components Penetration through the Skin. *Eur J Pharm Sci* **2021**, *160*, https://doi.org/10.1016/j.ejps.2021.105765.
46. Ehrlich, H.; Krajewska, B.; Hanke, T.; Born, R.; Heinemann, S.; Knieb, C.; Worch, H. Chitosan Membrane as a Template for Hydroxyapatite Crystal Growth in a Model Dual Membrane Diffusion System. *J. Membr. Sci.* **2006**, *273*, 124–128, https://doi.org/10.1016/j.memsci.2005.11.050.
47. Szatkowski, T.; Kołodziejczak-Radzimska, A.; Zdarta, J.; Szwarc-Rzepka, K.; Paukszta, D.; Wysokowski, M.; Ehrlich, H.; Jesionowski, T. Synthesis and Characterization of Hydroxyapatite/Chitosan Composites. *Physicochem. Probl. Miner. Process.* **2015**, *51*, 575–585, https://doi.org/10.5277/ppmp150217.
48. Stepniak, I.; Galinski, M.; Nowacki, K.; Wysokowski, M.; Jakubowska, P.; Bazhenov, V.V.; Leisegang, T.; Ehrlich, H.; Jesionowski, T. A Novel Chitosan/Sponge Chitin Origin Material as a Membrane for

Supercapacitors – Preparation and Characterization. *RSC Adv.* **2016**, *6*, 4007–4013, https://doi.org/10.1039/C5RA22047E.
49. Li, Q.; Mahendra, S.; Lyon, D.Y.; Brunet, L.; Liga, M.V.; Li, D.; Alvarez, P.J.J. Antimicrobial Nanomaterials for Water Disinfection and Microbial Control: Potential Applications and Implications. *Water Res.* **2008**, *42*, 4591–4602, https://doi.org/10.1016/j.watres.2008.08.015.
50. Bhatnagar, A.; Sillanpää, M. Applications of Chitin- and Chitosan-Derivatives for the Detoxification of Water and Wastewater — A Short Review. *Adv. Colloid Interface Sci.* **2009**, *152*, 26–38, https://doi.org/10.1016/j.cis.2009.09.003.
51. Renault, F.; Sancey, B.; Badot, P.-M.; Crini, G. Chitosan for Coagulation/Flocculation Processes – An Eco-Friendly Approach. *Eur. Polym. J.* **2009**, *45*, 1337–1348, https://doi.org/10.1016/j.eurpolymj.2008.12.027.
52. Babel, S.; Kurniawan, T.A. Low-Cost Adsorbents for Heavy Metals Uptake from Contaminated Water: A Review. *J. Hazard. Mater.* **2003**, *97*, 219–243, https://doi.org/10.1016/S0304-3894(02)00263-7.
53. Soares, J.M.A.; da Silva Júnior, E.D.; Oliveira de Veras, B.; Yara, R.; de Albuquerque, P.B.S.; de Souza, M.P. Active Biodegradable Film Based on Chitosan and Cenostigma Nordestinum' Extracts for Use in the Food Industry. *J Polym Environ* **2022**, *30*, 217–231, https://doi.org/10.1007/s10924-021-02192-5.
54. Babaei-Ghazvini, A.; Acharya, B.; Korber, D.R. Antimicrobial Biodegradable Food Packaging Based on Chitosan and Metal/Metal-Oxide Bio-Nanocomposites: A Review. *Polymers* **2021**, *13*, https://doi.org/10.3390/polym13162790.
55. Díaz-Montes, E.; Castro-Muñoz, R. Trends in Chitosan as a Primary Biopolymer for Functional Films and Coatings Manufacture for Food and Natural Products. *Polymers* **2021**, *13*, https://doi.org/10.3390/polym13050767.
56. Fonseca-García, A.; Jiménez-Regalado, E.J.; Aguirre-Loredo, R.Y. Preparation of a Novel Biodegradable Packaging Film Based on Corn Starch-Chitosan and Poloxamers. *Carbohydr. Polym.* **2021**, *251*, https://doi.org/10.1016/j.carbpol.2020.117009.
57. Yadav, S.; Mehrotra, G.K.; Dutta, P.K. Chitosan Based ZnO Nanoparticles Loaded Gallic-Acid Films for Active Food Packaging. *Food Chem.* **2021**, *334*, https://doi.org/10.1016/j.foodchem.2020.127605.
58. Kumirska, J.; Czerwicka, M.; Kaczyński, Z.; Bychowska, A.; Brzozowski, K.; Thöming, J.; Stepnowski, P. Application of Spectroscopic Methods for Structural Analysis of Chitin and Chitosan. *Mar Drugs* **2010**, *8*, 1567–1636, https://doi.org/10.3390/md8051567.
59. Woodward, A.E. Transitions in Polymers by Nuclear Magnetic Resonance a Study. *Polym. Eng. Sci.* **1962**, *2*, 86–91, https://doi.org/10.1002/pen.760020115.
60. Rinaudo, M.; Le Dung, P.; Gey, C.; Milas, M. Substituent Distribution on O,N-Carboxymethylchitosans by 1H and 13C n.m.r. *Int J Biol Macromol* **1992**, *14*, 122–128, https://doi.org/10.1016/s0141-8130(05)80001-7.
61. Heras, A.; Rodríguez, N.M.; Ramos, V.M.; Agulló, E. N-Methylene Phosphonic Chitosan: A Novel Soluble Derivative. *Carbohydr. Polym.* **2001**, *44*, 1–8, https://doi.org/10.1016/S0144-8617(00)00195-8.
62. Lopez, J.M.; Sánchez, L.F.; Nakamatsu, J.; Maruenda, H. Study of the Acetylation Pattern of Chitosan by Pure Shift NMR. *Anal. Chem.* **2020**, *92*, 12250–12256, https://doi.org/10.1021/acs.analchem.0c01638.
63. Facchinatto, W.M.; dos Santos Garcia, R.H.; dos Santos, D.M.; Fiamingo, A.; Menezes Flores, D.W.; Campana-Filho, S.P.; de Azevedo, E.R.; Colnago, L.A. Fast-Forward Approach of Time-Domain NMR Relaxometry for Solid-State Chemistry of Chitosan. *Carbohydr. Polym.* **2021**, *256*, https://doi.org/10.1016/j.carbpol.2020.117576.
64. Hirai, A.; Odani, H.; Nakajima, A. Determination of Degree of Deacetylation of Chitosan by 1H NMR Spectroscopy. *Polymer Bulletin* **1991**, *26*, 87–94, https://doi.org/10.1007/BF00299352.
65. Lavertu, M.; Xia, Z.; Serreqi, A.N.; Berrada, M.; Rodrigues, A.; Wang, D.; Buschmann, M.D.; Gupta, A. A Validated 1H NMR Method for the Determination of the Degree of Deacetylation of Chitosan. *J. Pharm. Biomed* **2003**, *32*, 1149–1158, https://doi.org/10.1016/S0731-7085(03)00155-9.
66. Weißpflog, J.; Vehlow, D.; Müller, M.; Kohn, B.; Scheler, U.; Boye, S.; Schwarz, S. Characterization of Chitosan with Different Degree of Deacetylation and Equal Viscosity in Dissolved and Solid State – Insights by Various Complimentary Methods. *Int. J. Biol. Macromol.* **2021**, *171*, 242–261, https://doi.org/10.1016/j.ijbiomac.2021.01.010.
67. Pérez-Álvarez, L.; Ruiz-Rubio, L.; Vilas-Vilela, J.L. Determining the Deacetylation Degree of Chitosan: Opportunities To Learn Instrumental Techniques. *J. Chem. Educ.* **2018**, *95*, 1022–1028, https://doi.org/10.1021/acs.jchemed.7b00902.
68. Kamari, A.; Yusoff, S.N.M. N-Octyl Chitosan Derivatives as Amphiphilic Carrier Agents for Herbicide Formulations. *Open Chemistry* **2019**, *17*, 365–380, https://doi.org/10.1515/chem-2019-0043.
69. Waseda, Y.; Matsubara, E.; Shinoda, K. *X-Ray Diffraction Crystallography*. 1st ed.; Springer Berlin Heidelberg: Berlin, Heidelberg, **2011**.
70. Kim, S.H.; Lee, C.M.; Kafle, K. Characterization of Crystalline Cellulose in Biomass: Basic Principles, Applications, and Limitations of XRD, NMR, IR, Raman, and SFG. *Korean J. Chem. Eng.* **2013**, *30*, 2127–2141, https://doi.org/10.1007/s11814-013-0162-0.
71. Qi, L.; Xu, Z.; Jiang, X.; Hu, C.; Zou, X. Preparation and Antibacterial Activity of Chitosan Nanoparticles. *Carbohydr. Res.* **2004**, *339*, 2693–2700, https://doi.org/10.1016/j.carres.2004.09.007.

72. Jampafuang, Y.; Tongta, A.; Waiprib, Y. Impact of Crystalline Structural Differences Between α- and β-Chitosan on Their Nanoparticle Formation Via Ionic Gelation and Superoxide Radical Scavenging Activities. *Polymers (Basel)* **2019**, *11*, https://doi.org/10.3390/polym11122010.
73. Matet, M.; Heuzey, M.-C.; Pollet, E.; Ajji, A.; Avérous, L. Innovative Thermoplastic Chitosan Obtained by Thermo-Mechanical Mixing with Polyol Plasticizers. *Carbohydr. Polym.* **2013**, *95*, 241–251, https://doi.org/10.1016/j.carbpol.2013.02.052.
74. Hejjaji, E.M.A.; Smith, A.M.; Morris, G.A. Designing Chitosan-Tripolyphosphate Microparticles with Desired Size for Specific Pharmaceutical or Forensic Applications. *Int. J. Biol. Macromol.* **2017**, *95*, 564–573, https://doi.org/10.1016/j.ijbiomac.2016.11.092.
75. Zhang, Y.; Xue, C.; Xue, Y.; Gao, R.; Zhang, X. Determination of the Degree of Deacetylation of Chitin and Chitosan by X-Ray Powder Diffraction. *Carbohydr. Res.* **2005**, *340*, 1914–1917, https://doi.org/10.1016/j.carres.2005.05.005.
76. Kaya, M.; Mujtaba, M.; Ehrlich, H.; Salaberria, A.M.; Baran, T.; Amemiya, C.T.; Galli, R.; Akyuz, L.; Sargin, I.; Labidi, J. On Chemistry of γ-Chitin. *Carbohydr. Polym.* **2017**, *176*, 177–186, https://doi.org/10.1016/j.carbpol.2017.08.076.
77. Zhang, K.; Geissler, A.; Fischer, S.; Brendler, E.; Bäucker, E. Solid-State Spectroscopic Characterization of α-Chitins Deacetylated in Homogeneous Solutions. *J. Phys. Chem. B* **2012**, *116*, 4584–4592, https://doi.org/10.1021/jp210469x.
78. Kumar, S.; Koh, J. Physiochemical, Optical and Biological Activity of Chitosan-Chromone Derivative for Biomedical Applications. *Int. J. Mol. Sci.* **2012**, *13*, 6102–6116, https://doi.org/10.3390/ijms13056102.
79. Choi, C.Y.; Kim, S.B.; Pak, P.K.; Yoo, D.I.; Chung, Y.S. Effect of N-Acylation on Structure and Properties of Chitosan Fibers. *Carbohydr. Polym.* **2007**, *68*, 122–127, https://doi.org/10.1016/j.carbpol.2006.07.018.
80. Fan, M.; Hu, Q.; Shen, K. Preparation and Structure of Chitosan Soluble in Wide PH Range. *Carbohydr. Polym.* **2009**, *78*, 66–71, https://doi.org/10.1016/j.carbpol.2009.03.031.
81. Zhang, W.; Zhang, J.; Jiang, Q.; Xia, W. Physicochemical and Structural Characteristics of Chitosan Nanopowders Prepared by Ultrafine Milling. *Carbohydr. Polym.* **2012**, *87*, 309–313, https://doi.org/10.1016/j.carbpol.2011.07.057.
82. Stevie, F.A.; Donley, C.L. Introduction to X-Ray Photoelectron Spectroscopy. *J. Vac. Sci. Technol. A* **2020**, *38*, https://doi.org/10.1116/6.0000412.
83. Dambies, L.; Guimon, C.; Yiacoumi, S.; Guibal, E. Characterization of Metal Ion Interactions with Chitosan by X-Ray Photoelectron Spectroscopy. *Colloids Surf. A: Physicochem. Eng. Asp.* **2000**, *177*, 203–214, https://doi.org/10.1016/S0927-7757(00)00678-6.
84. Varma, A.J.; Deshpande, S.V.; Kennedy, J.F. Metal Complexation by Chitosan and Its Derivatives: A Review. *Carbohydr. Polym.* **2004**, *55*, 77–93, https://doi.org/10.1016/j.carbpol.2003.08.005.
85. Lawrie, G.; Keen, I.; Drew, B.; Chandler-Temple, A.; Rintoul, L.; Fredericks, P.; Grøndahl, L. Interactions between Alginate and Chitosan Biopolymers Characterized Using FTIR and XPS. *Biomacromolecules* **2007**, *8*, 2533–2541, https://doi.org/10.1021/bm070014y.
86. Li, P.-C.; Liao, G.; Kumar, Dr.S.R.; Shih, C.-M.; Yang, C.-C.; Wang, D.-M.; Lue, S. Fabrication and Characterization of Chitosan Nanoparticle-Incorporated Quaternized Poly(Vinyl Alcohol) Composite Membranes as Solid Electrolytes for Direct Methanol Alkaline Fuel Cells. *Electrochim. Acta* **2015**, *187*, https://doi.org/10.1016/j.electacta.2015.11.117.
87. Varan, N.Y. Characterization of Chitosan Particles via Attenuated Total Reflection Fourier Transform Infrared Spectroscopy, Conductometric Titration, Viscosity Average Molecular Weight and X-Ray Photoelectron Spectroscopy. *Asian J. Chem.* **2017**, *29*, 825–828, https://doi.org/10.14233/ajchem.2017.20324.
88. Rubina, M.S.; Elmanovich, I.V.; Shulenina, A.V.; Peters, G.S.; Svetogorov, R.D.; Egorov, A.A.; Naumkin, A.V.; Vasil'kov, A.Y. Chitosan Aerogel Containing Silver Nanoparticles: From Metal-Chitosan Powder to Porous Material. *Polym. Test.* **2020**, *86*, https://doi.org/10.1016/j.polymertesting.2020.106481.
89. Jiang, H.; Liang, J.; Grant, J.; Su, W.; Bunning, T.; Cooper, T.; Adams, W. Characterization of Chitosan and Rare-earth-metal-ion Doped Chitosan Films. *Macromol Chem Phys* **2003**, *198*, 1561–1578, https://doi.org/10.1002/macp.1997.021980519.
90. Butnariu, M. The Study of Infrared Spectrum of Chitin and Chitosan Extract as Potential Sources of Biomass. *Dig. J. Nanomater. Biostructures* **2015**, *10*, 1129–1138.
91. Yuan, Y.; Li, H.; Leite, W.; Zhang, Q.; Bonnesen, P.V.; Labbé, J.L.; Weiss, K.L.; Pingali, S.V.; Hong, K.; Urban, V.S.; Salmon, S.; O'Neill, H. Biosynthesis and characterization of deuterated chitosan in filamentous fungus and yeast. *Carbohydrate Polymers* **2021**, *257*, https://doi.org/10.1016/j.carbpol.2021.117637.
92. Zam, Z.; Muin, F.; Fataruba, A. Identification of Chitosan Beads from Coconut Crab Patani Variety Using Fourier Transform Infrared Spectroscopy (FTIR). *J. Phys. Conf. Ser.* **2021**, *1832*, https://doi.org/10.1088/1742-6596/1832/1/012014.
93. Brugnerotto, J.; Lizardi, J.; Goycoolea, F.M.; Argüelles-Monal, W.; Desbrières, J.; Rinaudo, M. An Infrared Investigation in Relation with Chitin and Chitosan Characterization. *Polymer* **2001**, *42*, 3569–3580, https://doi.org/10.1016/S0032-3861(00)00713-8.

94. Hajji, S.; Younes, I.; Ghorbel-Bellaaj, O.; Hajji, R.; Rinaudo, M.; Nasri, M.; Jellouli, K. Structural Differences between Chitin and Chitosan Extracted from Three Different Marine Sources. *Int. J. Biol. Macromol.* **2014**, *65*, 298–306, https://doi.org/10.1016/j.ijbiomac.2014.01.045.
95. Van de Velde, K.; Kiekens, P. Structure Analysis and Degree of Substitution of Chitin, Chitosan and Dibutyrylchitin by FT-IR Spectroscopy and Solid State 13C NMR. *Carbohydr. Polym.* **2004**, *58*, 409–416, https://doi.org/10.1016/j.carbpol.2004.08.004.
96. Carson, L.; Kelly-Brown, C.; Stewart, M.; Oki, A.; Regisford, G.; Luo, Z.; Bakhmutov, V.I. Synthesis and Characterization of Chitosan–Carbon Nanotube Composites. *Mater Lett* **2009**, *63*, 617–620, https://doi.org/10.1016/j.matlet.2008.11.060.
97. Kurita, K.; Ikeda, H.; Yoshida, Y.; Shimojoh, M.; Harata, M. Chemoselective Protection of the Amino Groups of Chitosan by Controlled Phthaloylation: Facile Preparation of a Precursor Useful for Chemical Modifications. *Biomacromolecules* **2002**, *3*, 1–4, https://doi.org/10.1021/bm0101163.
98. Bumbrah, G.S.; Sharma, R.M. Raman Spectroscopy – Basic Principle, Instrumentation and Selected Applications for the Characterization of Drugs of Abuse. *Egypt. J. Forensic Sci.* **2016**, *6*, 209–215, https://doi.org/10.1016/j.ejfs.2015.06.001.
99. Babatunde, E.; O. Ighalo, J.; Akolo, S.; Adeniyi, A.; Adepoju, L. Investigation of Biomaterial Characteristics of Chitosan Produced from Crab Shells. *Materials International* **2020**, *2*, 303-310.
100. Ren, X.D.; Liu, Q.S.; Feng, H.; Yin, X.Y. The Characterization of Chitosan Nanoparticles by Raman Spectroscopy. *Appl. Mech. Mater.* **2014**, *665*, 367–370, https://doi.org/10.4028/www.scientific.net/AMM.665.367.
101. Zając, A.; Hanuza, J.; Wandas, M.; Dymińska, L. Determination of N-Acetylation Degree in Chitosan Using Raman Spectroscopy. *Spectrochim. Acta A Mol. Biomol. Spectrosc.* **2015**, *134*, 114–120, https://doi.org/10.1016/j.saa.2014.06.071.
102. Thamilarasan, V.; Sethuraman, V.; Gopinath, K.; Balalakshmi, C.; Govindarajan, M.; Mothana, R.; Siddiqui, N.; Khaled, J.; Benelli, G. Single Step Fabrication of Chitosan Nanocrystals Using Penaeus Semisulcatus: Potential as New Insecticides, Antimicrobials and Plant Growth Promoters. *J. Clust. Sci.* **2018**, *29*, https://doi.org/10.1007/s10876-018-1342-1.
103. Wu, T.; Zivanovic, S. Determination of the Degree of Acetylation (DA) of Chitin and Chitosan by an Improved First Derivative UV Method. *Carbohydr. Polym.* **2008**, *2*, 248–253, https://doi.org/10.1016/j.carbpol.2007.11.024.
104. Jia, X.; Chen, X.; Xu, Z. Spectrophotometric Determination of Chitosan with Cibacron Brilliant Red 3B-A. *Chinese Journal of Pharmaceutical Analysis* **2009**, *29*, 1726–1728.
105. Wischke, C.; Borchert, H.-H. Increased Sensitivity of Chitosan Determination by a Dye Binding Method. *Carbohydr Res* **2006**, *341*, 2978–2979, https://doi.org/10.1016/j.carres.2006.10.012.
106. Mendelovits, A.; Prat, T.; Gonen, Y.; Rytwo, G. Improved Colorimetric Determination of Chitosan Concentrations by Dye Binding. *Appl Spectrosc* **2012**, *66*, 979–982, https://doi.org/10.1366/12-06591a.
107. Mattai, J.; Hayes, E.R. Characterization of Chitosan by Pyrolysis—Mass Spectrometry. *J Anal Appl Pyrolysis* **1982**, *3*, 327–334, https://doi.org/10.1016/0165-2370(82)80019-3.
108. Muzzarelli, R.A.A. Colorimetric Determination of Chitosan. *Anal. Biochem.* **1998**, *260*, 255–257, https://doi.org/10.1006/abio.1998.2705.
109. Badawy, M.E.I. A New Rapid and Sensitive Spectrophotometric Method for Determination of a Biopolymer Chitosan. *Int. J. Carbohydr. Chem.* **2012**, *2012*, 1–7, https://doi.org/10.1155/2012/139328.
110. Mojumdar, A.; Upadhyay, A.K.; Raina, V.; Ray, L. A Simple and Rapid Colorimetric Method for the Estimation of Chitosan Produced by Microbial Degradation of Chitin Waste. *J. Microbiol. Methods* **2019**, *158*, 66–70, https://doi.org/10.1016/j.mimet.2019.02.001.
111. Larionova, N.I.; Zubaerova, D.K.; Guranda, D.T.; Pechyonkin, M.A.; Balabushevich, N.G. Colorimetric Assay of Chitosan in Presence of Proteins and Polyelectrolytes by Using O-Phthalaldehyde. *Carbohydr. Polym.* **2009**, *4*, 724–727, https://doi.org/10.1016/j.carbpol.2008.10.009.
112. Abou-Shoer, M. A Simple Colorimetric Method for the Evaluation of Chitosan. *Am. J. Anal. Chem.* **2010**, *1*, 91–94, https://doi.org/10.4236/ajac.2010.12012.
113. Lago, M.A.; Rodríguez Bernaldo de Quirós, A.; Sendón, R.; Sanches-Silva, A.; Costa, H.S.; Sánchez-Machado, D.I.; López-Cervantes, J.; Soto Valdez, H.; Aurrekoetxea, G.P.; Angulo, I.; Paseiro Losada, P. Compilation of analytical methods to characterize and determine chitosan, and main applications of the polymer in food active packaging Recopilación de métodos analíticos para la caracterización y determinación del quitosano y las principales aplicaciones del polímero en los envases activos alimentarios. *CyTA - Journal of Food* **2011**, *9*, 319-328, https://doi.org/10.1080/19476337.2011.603844.
114. Wu, S.H.; Hu, S.Y.; Huang, G.D.; Pan, W.S.; Yu, C.L.; Tan, S.R.; Chen, S.D.; Su, Z.Q. Experimental Investigation on Determination of Chitosan by Spectrophotometry. *Adv Mat Res* **2012**, *554–556*, 1895–1900, https://doi.org/10.4028/www.scientific.net/AMR.554-556.1895.
115. Chitosan Assay Kit (Colorimetric) (Ab273338) | Abcam Available online: https://www.abcam.com/chitosan-assay-kit-colorimetric-ab273338.html (accessed on 10 May 2022).
116. Chitosan Colorimetric Assay Kit | K995 | BioVision, Inc. Available online: https://www.biovision.com/chitosan-colorimetric-assay-kit.html (accessed on 10 May 2022).

117. Helaluddin, A.; Khalid, R.S.; Alaama, M.; Abbas, S.A. Main Analytical Techniques Used for Elemental Analysis in Various Matrices. *Trop. J. Pharm Res* **2016**, *15*, https://doi.org/10.4314/tjpr.v15i2.29.
118. dos Santos, Z.M.; Caroni, A.L.P.F.; Pereira, M.R.; da Silva, D.R.; Fonseca, J.L.C. Determination of Deacetylation Degree of Chitosan: A Comparison between Conductometric Titration and CHN Elemental Analysis. *Carbohydr. Res.* **2009**, *344*, 2591–2595, https://doi.org/10.1016/j.carres.2009.08.030.
119. Sarwar, A.; Katas, H.; Samsudin, S.; Zin, N. Regioselective Sequential Modification of Chitosan via Azide-Alkyne Click Reaction: Synthesis, Characterization, and Antimicrobial Activity of Chitosan Derivatives and Nanoparticles. *PLOS ONE* **2015**, *10*, https://doi.org/10.1371/journal.pone.0123084.
120. Kasaai, M.R. Various Methods for Determination of the Degree of N-Acetylation of Chitin and Chitosan: A Review. *J Agric Food Chem* **2009**, *57*, 1667–1676, https://doi.org/10.1021/jf803001m.
121. Gill, P.; Moghadam, T.T.; Ranjbar, B. Differential Scanning Calorimetry Techniques: Applications in Biology and Nanoscience. *J Biomol Tech* **2010**, *21*, 167–193.
122. Corazzari, I.; Nisticò, R.; Turci, F.; Faga, M.G.; Franzoso, F.; Tabasso, S.; Magnacca, G. Advanced Physico-Chemical Characterization of Chitosan by Means of TGA Coupled on-Line with FTIR and GCMS: Thermal Degradation and Water Adsorption Capacity. *Polym. Degrad. Stab.* **2015**, *112*, 1–9, https://doi.org/10.1016/j.polymdegradstab.2014.12.006.
123. Kocabay, S.; Bahar, M.R.; Tekin, S.; Akkaya, R.; Akkaya, B. Chemical and Biological Characterization of Sulfated Chitosan Oligomer as Heparin Mimics. *Polym. Polym. Compos.* **2021**, *29*, S1023–S1032, https://doi.org/10.1177/09673911211035068.
124. Kittur, F.S.; Harish Prashanth, K.V.; Udaya Sankar, K.; Tharanathan, R.N. Characterization of Chitin, Chitosan and Their Carboxymethyl Derivatives by Differential Scanning Calorimetry. *Carbohydr. Polym.* **2002**, *49*, 185–193, https://doi.org/10.1016/S0144-8617(01)00320-4.
125. Bagheri, B.; Zarrintaj, P.; Surwase, S.S.; Baheiraei, N.; Saeb, M.R.; Mozafari, M.; Kim, Y.C.; Park, O.O. Self-Gelling Electroactive Hydrogels Based on Chitosan–Aniline Oligomers/Agarose for Neural Tissue Engineering with on-Demand Drug Release. *Colloids Surf. B* **2019**, *184*, https://doi.org/10.1016/j.colsurfb.2019.110549.
126. Menczel, J.D.; Prime, R.B. *Thermal Analysis of Polymers: Fundamentals and Applications*. Menczel, J.D.; Prime, R.B. Eds.; John Wiley: Hoboken, N.J, **2009.**
127. Hosseini, S.F.; Zandi, M.; Rezaei, M.; Farahmandghavi, F. Two-Step Method for Encapsulation of Oregano Essential Oil in Chitosan Nanoparticles: Preparation, Characterization and in Vitro Release Study. *Carbohydr. Polym.* **2013**, *95*, 50–56, https://doi.org/10.1016/j.carbpol.2013.02.031.
128. Liao, S.-K.; Hung, C.-C.; Lin, M.-F. A Kinetic Study of Thermal Degradations of Chitosan/Polycaprolactam Blends. *Macromol. Res.* **2004**, *12*, 466–473, https://doi.org/10.1007/BF03218428.
129. Fang, Y.; Zhang, R.; Duan, B.; Liu, M.; Lu, A.; Zhang, L. Recyclable Universal Solvents for Chitin to Chitosan with Various Degrees of Acetylation and Construction of Robust Hydrogels. *ACS Sustainable Chem. Eng.* **2017**, *5*, 2725–2733, https://doi.org/10.1021/acssuschemeng.6b03055.
130. Bird, I.M. High Performance Liquid Chromatography: Principles and Clinical Applications. *BMJ* **1989**, *299*, 783–787, https://doi.org/10.1136/bmj.299.6702.783.
131. Miao, Q.; Cui, Y.; Zhang, J.; Mi, Y.; Tan, W.; Li, Q.; Gu, G.; Dong, F.; Guo, Z. Determination of Chitosan Content with Ratio Coefficient Method and HPLC. *Int. J. Biol. Macromol.* **2020**, *164*, 384–388, https://doi.org/10.1016/j.ijbiomac.2020.07.013.
132. Ng, C.-H.; Hein, S.; Chandrkrachang, S.; Stevens, W.F. Evaluation of an Improved Acid Hydrolysis-HPLC Assay for the Acetyl Content in Chitin and Chitosan. *J Biomed Mater Res B Appl Biomater* **2006**, *76*, 155–160, https://doi.org/10.1002/jbm.b.30353.
133. Miao, Q.; Mi, Y.; Cui, J.; Zhang, J.; Tan, W.; Li, Q.; Guo, Z. Determination of Chitosan Content with Schiff Base Method and HPLC. *Int. J. Biol. Macromol.* **2021**, *182*, 1537–1542, https://doi.org/10.1016/j.ijbiomac.2021.05.121.
134. Eikenes, M.; Fongen, M.; Roed, L.; Stenstrøm, Y. Determination of Chitosan in Wood and Water Samples by Acidic Hydrolysis and Liquid Chromatography with Online Fluorescence Derivatization. *Carbohydr. Polym.* **2005**, *61*, 29–38, https://doi.org/10.1016/j.carbpol.2005.02.006.
135. Wattjes, J.; Niehues, A.; Cord-Landwehr, S.; Hoßbach, J.; David, L.; Delair, T.; Moerschbacher, B.M. Enzymatic Production and Enzymatic-Mass Spectrometric Fingerprinting Analysis of Chitosan Polymers with Different Nonrandom Patterns of Acetylation. *J. Am. Chem. Soc.* **2019**, *141*, 3137–3145, https://doi.org/10.1021/jacs.8b12561.
136. Subramanyam, C.; Saligame, R. An Enzymic Method for the Determination of Chitin and Chitosan in Fungal Cell Walls. *J. Biosci.* **1987**, *12*, 125–129, https://doi.org/10.1007/BF02702963.
137. Nanjo, F.; Katsumi, R.; Sakai, K. Enzymatic Method for Determination of the Degree of Deacetylation of Chitosan. *Anal. Biochem.* **1991**, *193*, 164–167, https://doi.org/10.1016/0003-2697(91)90002-B.
138. Wiener, J.; MacHanňová, D.; Müllerová, J.; Krátký, O. Analytical Methods for Chitosan. *J. Nat. Fibers* **2006**, *3*, 229–240, https://doi.org/10.1300/J395v03n02_15.
139. Binnewerg, B.; Schubert, M.; Voronkina, A.; Muzychka, L.; Wysokowski, M.; Petrenko, I.; Djurović, M.; Kovalchuk, V.; Tsurkan, M.; Martinovic, R.; Bechmann, N.; Fursov, A.; Ivanenko, V.N.; Tabachnick, K.R.; Smolii, O.B.; Joseph, Y.; Giovine, M.; Bornstein, S.R.; Stelling, A.L.; Tunger, A.; Schmitz, M.; Taniya,

O.S.; Kovalev, I.S.; Zyryanov, G.V.; Guan, K.; Ehrlich, H. Marine Biomaterials: Biomimetic and Pharmacological Potential of Cultivated Aplysina Aerophoba Marine Demosponge. *Mater. Sci. Eng. C.* **2020**, *109*, https://doi.org/10.1016/j.msec.2019.110566.

140. Ehrlich, H.; Ilan, M.; Maldonado, M.; Muricy, G.; Bavestrello, G.; Kljajic, Z.; Carballo, J.L.; Schiaparelli, S.; Ereskovsky, A.; Schupp, P.; Born, R.; Worch, H.; Bazhenov, V.V.; Kurek, D.; Varlamov, V.; Vyalikh, D.; Kummer, K.; Sivkov, V.V.; Molodtsov, S.L.; Meissner, H.; Richter, G.; Steck, E.; Richter, W.; Hunoldt, S.; Kammer, M.; Paasch, S.; Krasokhin, V.; Patzke, G.; Brunner, E. Three-Dimensional Chitin-Based Scaffolds from Verongida Sponges (Demospongiae: Porifera). Part I. Isolation and Identification of Chitin. *Int. J. Biol. Macromol.* **2010**, *47*, 132–140, https://doi.org/10.1016/j.ijbiomac.2010.05.007.
141. Ehrlich, H.; Steck, E.; Ilan, M.; Maldonado, M.; Muricy, G.; Bavestrello, G.; Kljajic, Z.; Carballo, J.L.; Schiaparelli, S.; Ereskovsky, A.; Schupp, P.; Born, R.; Worch, H.; Bazhenov, V.V.; Kurek, D.; Varlamov, V.; Vyalikh, D.; Kummer, K.; Sivkov, V.V.; Molodtsov, S.L.; Meissner, H.; Richter, G.; Hunoldt, S.; Kammer, M.; Paasch, S.; Krasokhin, V.; Patzke, G.; Brunner, E.; Richter, W. Three-Dimensional Chitin-Based Scaffolds from Verongida Sponges (Demospongiae: Porifera). Part II: Biomimetic Potential and Applications. *Int. J. Biol. Macromol.* **2010**, *47*, 141–145, https://doi.org/10.1016/j.ijbiomac.2010.05.009.
142. Fromont, J.; Żółtowska-Aksamitowska, S.; Galli, R.; Meissner, H.; Erpenbeck, D.; Vacelet, J.; Diaz, C.; Tsurkan, M.V.; Petrenko, I.; Youssef, D.T.A.; Ehrlich, H. New Family and Genus of a Dendrilla-like Sponge with Characters of Verongiida. Part II. Discovery of Chitin in the Skeleton of Ernstilla Lacunosa. *Zool. Anz.* **2019**, *280*, 21–29, https://doi.org/10.1016/j.jcz.2019.03.002.
143. Kertmen, A.; Petrenko, I.; Schimpf, C.; Rafaja, D.; Petrova, O.; Sivkov, V.; Nekipelov, S.; Fursov, A.; Stelling, A.L.; Heimler, K.; Rogoll, A.; Vogt, C.; Ehrlich, H. Calcite Nanotuned Chitinous Skeletons of Giant Ianthella Basta Marine Demosponge. *Int. J. Mol. Sci.* **2021**, *22*, https://doi.org/10.3390/ijms222212588.
144. Kovalchuk, V.; Voronkina, A.; Binnewerg, B.; Schubert, M.; Muzychka, L.; Wysokowski, M.; Tsurkan, M.V.; Bechmann, N.; Petrenko, I.; Fursov, A.; Martinovic, R.; Ivanenko, V.N.; Fromont, J.; Smolii, O.B.; Joseph, Y.; Giovine, M.; Erpenbeck, D.; Gelinsky, M.; Springer, A.; Guan, K.; Bornstein, S.R.; Ehrlich, H. Naturally Drug-Loaded Chitin: Isolation and Applications. *Mar Drugs* **2019**, *17*, https://doi.org/10.3390/md17100574.
145. Schubert, M.; Binnewerg, B.; Voronkina, A.; Muzychka, L.; Wysokowski, M.; Petrenko, I.; Kovalchuk, V.; Tsurkan, M.; Martinovic, R.; Bechmann, N.; Ivanenko, V.N.; Fursov, A.; Smolii, O.B.; Fromont, J.; Joseph, Y.; Bornstein, S.R.; Giovine, M.; Erpenbeck, D.; Guan, K.; Ehrlich, H. Naturally Prefabricated Marine Biomaterials: Isolation and Applications of Flat Chitinous 3D Scaffolds from Ianthella Labyrinthus (Demospongiae: Verongiida). *Int. J. Mol. Sci.* **2019**, *20*, https://doi.org/10.3390/ijms20205105.
146. Vacelet, J.; Erpenbeck, D.; Diaz, C.; Ehrlich, H.; Fromont, J. New Family and Genus for Dendrilla-like Sponges with Characters of Verongiida. Part I Redescription of Dendrilla Lacunosa Hentschel 1912, Diagnosis of the New Family Ernstillidae and Ernstilla n. g. *Zool. Anz.* **2019**, *280*, 14–20, https://doi.org/10.1016/j.jcz.2019.03.001.
147. Khrunyk, Y.; Lach, S.; Petrenko, I.; Ehrlich, H. Progress in Modern Marine Biomaterials Research. *Mar. Drugs* **2020**, *18*, https://doi.org/10.3390/md18120589.
148. Muzychka, L.; Voronkina, A.; Kovalchuk, V.; Smolii, O.B.; Wysokowski, M.; Petrenko, I.; Youssef, D.T.A.; Ehrlich, I.; Ehrlich, H. Marine Biomimetics: Bromotyrosines Loaded Chitinous Skeleton as Source of Antibacterial Agents. *Appl. Phys. A* **2021**, *127*, https://doi.org/10.1007/s00339-020-04167-0.